OPTIMIZING LIGHT COLLECTION FROM THIN SCINTILLATORS USED IN A BETA-RAY CAMERA FOR SURGICAL USE

C. S. Levin, *L. R. MacDonald, M.P. Tornai, E.J. Hoffman, *J. Park
*Division of Nuclear Medicine & Biophysics, UCLA School of Medicine, and *Department of Physics, UCLA*

Abstract

We are developing a 1-2 cm^2 area camera for imaging the distribution of beta-emitting radiopharmaceuticals at the surface of tissue exposed during surgery. The front end consists of a very thin continuous or segmented scintillator sensitive to betas (positrons or electrons) of a few hundred keV, yet insensitive to gamma rays. The light from the scintillator is piped through clear fibers to the photon detector (PD). This approach requires that a sufficient number of scintillation photons be transported from the scintillator, through the fibers to the PD. The scintillator, reflector, surface treatments, geometry, fiber light guides, and optical couplings must be optimized. We report here on efforts made to optimize the light collection from < 3 mm thick plastic and $CaF_2(Eu)$ scintillators into clear fibers using experimental measurements and computer simulations. We measured that with a 1.25 cm diameter, 0.5 mm thick optimized $CaF_2(Eu)$ disk coupled to a 5 cm long bundle of clear optical fibers, on average, ~250 photoelectrons are produced at a PMT photocathode for a ^{204}Tl beta flood source (E_{max} = 763 keV). This corresponds to a sufficient number of photoelectrons for < 1 mm resolution imaging capabilities for the proposed camera.

I. INTRODUCTION

The surgical removal of a tumor is complicated in that usually only the bulk of the tumor is readily identified and removed, and the edges and fine extensions into normal tissue are difficult to detect. Currently the analysis of these tumor margins around the surgical cavity is done with multiple biopsies, which is time consuming, expensive and generally under samples the exposed tissue. We are developing an intra-operative beta-ray sensitive scintillation camera for improved detection of this residual malignant tissue using positron-labeled radiopharmaceuticals. We designed the instrument to be sensitive to beta particles (e.g. positrons from an ^{18}F-labeled radio-pharmaceutical, E_{max} = 635 keV), yet relatively insensitive to accompanying background annihilation photons. The imaging probe detector head consists of a low Z, low density, very thin, segmented or continuous scintillator (see Figure 1). The sensitive area of the face of the device exposed to the radioactive tissue is designed to be circular and roughly 1-2 cm^2. The short range of the betas in tissue and scintillator, close proximity to the area being imaged and relatively large area of the device ensure high image resolution and high sensitivity to beta emitting tissue at the surface of the cavity. Imaging capabilities help to distinguish signal from background and allow a relatively large area to be assayed in a short amount of time.

We previously developed a prototype device for feasibility studies using a discrete array of plastic scintillators coupled through fiber optics to multiple Visible Light Photon Counters (VLPCs) [1,2]. In addition to optimizing that system we are currently developing a similar instrument utilizing a multi-anode photomultiplier tube (PMT) [3,4]. We report here on efforts made to optimize the light collection from scintillators for the probe front-end, using computer simulations and experimental measurements with a bialkali PMT. We emphasize that although specific scintillators and geometries are studied in this work, many of the results obtained apply to a wide variety of system designs that utilize fiber optic readout of scintillators.

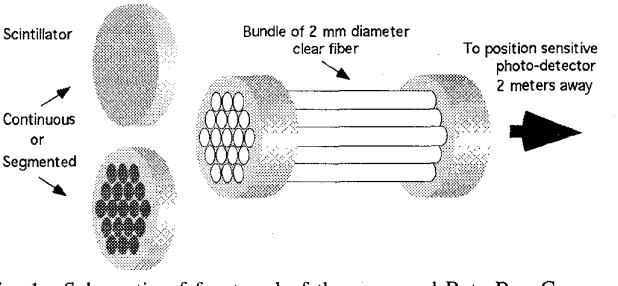

Fig. 1. Schematic of front end of the proposed Beta-Ray Camera. For flexibility, the scintillation light will be guided by a second-stage bundle of smaller diameter (< 1 mm) fibers (not shown). The total scintillator diameter is ~ 1.25 cm and the clear fiber bundle front end will be 5 cm long.

II. MATERIALS AND METHODS

A schematic of the device is shown in Figure 1. For flexibility and electrical insulation from body tissues during surgery, the light from the scintillator will be piped away from the patient through a matrix of long (~2 m), clear plastic optical fibers (not shown) into the multi-channel photon detector of choice (e.g. PMT, Avalanche Photodiode (APD), VLPC). An intermediate fiber bundle (seen in the figure) will be used to readout the light from the scintillators and transfer it to the long bundle. This will allow for a removable front end of the camera to accommodate a variety of imaging conditions with different front end geometries.

Positioning for the continuous scintillator version of the camera requires light sharing among the fibers, which will be accomplished with a suitable light diffuser between the scintillator and fibers. This design essentially miniaturizes the Anger camera concept and uses it for beta imaging without a collimator.

The challenge of this entire approach is to transport a sufficient number of scintillation photons from the scintillator, through the two stages of clear fiber and into the photo-detector. This involves optimizing such factors as the reflector, surface treatment, and the geometry of the scintillator, choice of clear fiber, couplings between these two

0018-9499/96$05.00

components and type of position sensitive photo-detector.

The choice of the low Z, low density scintillator will depend on light output and background considerations. We have focused our studies on relatively high light output plastic scintillators, such as, Bicron BC404 (un-clad, polyvinyl toluene (PVT) base) or BCF-10 scintillating fiber (with optical cladding), and $CaF_2(Eu)$. The properties of these scintillators are shown in Table 1. The segmented detector (Fig. 1, left, bottom) is a hexagonal matrix of 19 short, 2 mm diameter scintillator disks, and the continuous detector (Fig. 1, left, top), a 1.25 cm diameter disk. Improving the light yield in plastic by increasing the fluor concentration was investigated in [5].

Light output as a function of scintillator thickness was studied for both the large and small scintillator diameters. All of the measurements were performed inside a light tight box. The thinner the scintillator, the lower the gamma-ray background, however, too thin a material will not stop the average ^{18}F positron. Since we do not want sensitivity to background annihilation gamma rays in our light yield studies, we chose an electron (^{204}Tl) rather than positron (^{18}F) beta decay source for the experiments. The resulting light yield and energy resolution of the system are due to a convolution of energy deposition in the scintillator and transmission of light out of the scintillator, through the fiber bundles to the photodetector (PD).

Monte Carlo simulations were performed to study beta trajectories, scintillator light transmission and internal annihilation background in the scintillators of interest. The electron trajectory code was developed at UCLA, the optical photon tracking code used was DETECT [6], and EGS4 [7] was used to calculate the gamma-ray background.

Table 1. Properties of investigated low Z, low density scintillators for beta detection.

Scintil-lator	Light Output, (photons /MeV)	Max Wvlgth. Emission (nm)	Main Decay Constant (ns)	Bulk Light Attn. Length (cm)	Refractive Index	Effective Z	Density (g/cm^3)
BCF-10	8,000	432	2.7	190	1.6 core 1.49 clad	6.6	1.05
BC404	10,000	408	1.8	160	1.58	6.6	1.04
$CaF_2(Eu)$	17,000	435	940	~3-5	1.44	16.9	3.19

III. RESULTS

A. Monte Carlo Simulations: Electron Interactions and Background

$CaF_2(Eu)$ has nearly a factor of two higher light output than BC404, but from Monte Carlo simulations using the EGS4 code, above a 100 keV threshold, has three times the expected gamma ray background rate (from ^{18}F positron annihilation in the scintillator and subsequent Compton scatter) than does the same size of BC404 (PVT). However, because of its higher effective Z and density, the average thickness of the $CaF_2(Eu)$ required to stop an ^{18}F positron (E_{max} = 635 keV) is nearly one quarter of that required for PVT. The annihilation background in $CaF_2(Eu)$ will not be as severe for thinner dimensions.

Figure 2 shows a plot of the probability that betas deposit all of their energy vs scintillator thickness for ^{204}Tl and ^{18}F flood beta sources in $CaF_2(Eu)$ and plastic using Monte Carlo simulations of positron trajectories. The thickness required to completely encompass an average beta trajectory for a flood source (normal incidence) of radiation is an upper limit for that required to stop betas entering from all angles. From Figure 2 it is seen that the thickness required to completely absorb greater than 90% of ^{18}F positrons is 1.3 mm and 0.5 mm for PVT and CaF_2,(Eu), respectively. This thickness is on average 10% greater for the ^{204}Tl source than for the ^{18}F source. The average range of the positrons in these materials is 0.4 and 0.16 mm, respectively, which gives an estimate of the ultimate limit of the intrinsic resolution attainable with ^{18}F beta-ray imaging in those scintillators (in our fiber-coupled system we are "starved" for light so we want scintillator thicknesses consistent with complete absorption of the beta energy). Figure 3 shows simulated ^{204}Tl electron and ^{18}F positron trajectories in $CaF_2(Eu)$. Betas continuously deposit their energy through multiple scattering with approximately 1/3 of the total energy deposited at the end of its track, where large angle scatters occur.

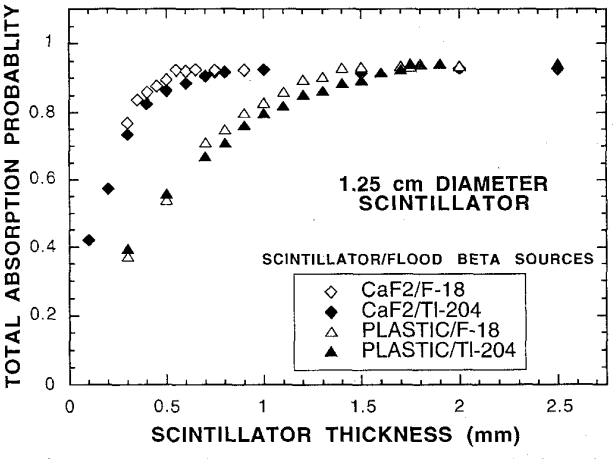

Fig. 2. Total absorption probability for beta events (trajectories) from ^{18}F and ^{204}Tl sources in $CaF_2(Eu)$ and plastic scintillators (a 1.25 cm diameter detector is assumed).

B. Monte Carlo Simulations: Scintillation Light Transmission

We are fortunate in the design of the imaging array that the scintillators used are very thin. For thin scintillators, where the cross-sectional area to thickness (length) ratio is high, it is much easier to collect the scintillation light from one end since the number of interactions with the sides is low. In fact, a good portion of the light may not undergo any reflections at all before exiting the scintillator. In regard to scintillation light yield, six aspects are presented: (1) the scintillator surface treatments, (2) the scintillator thickness, (3) the index of refraction of the coupling compounds used at interfaces, (4) the fiber numerical aperture, (5) the continuous scintillator's light diffuser refractive index and (6) reflective properties of the fiber holders (see Figure 1).

The surface treatment of the scintillators is important. External reflectors on the back side direct the light back into

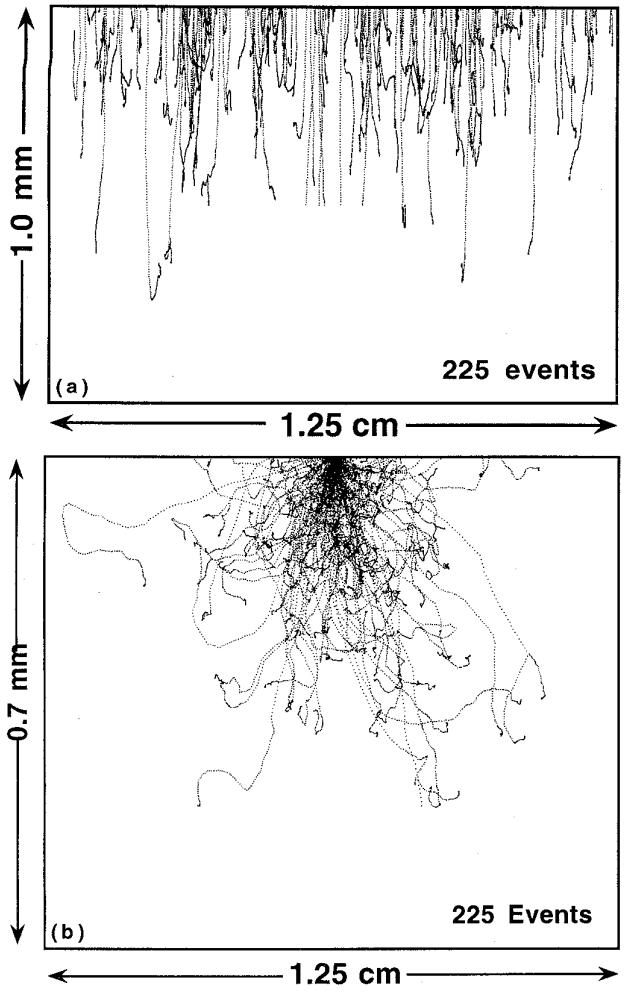

Fig. 3. Two dimensional plot (not to scale) of a Monte Carlo simulation of electron trajectories in $CaF_2(Eu)$ for (a) ^{204}Tl (E_{max} =765 keV) flood source and (b) ^{18}F (E_{max} =635 keV) point source at top center of scintillator. Note the effect of multiple scattering in the beta trajectories. The figures are not to scale.

the scintillator. Diffuse reflectors exhibit a Lambertian (cosθ) distribution where the reflected light is preferentially directed normal to the surface. Ground surfaces tend to break up internal reflections. Highly polished (specular) surfaces may trap some light due to internal reflections and this light may never enter the fiber light guides. This suggests that we may want a ground top surface with a diffuse reflector. Simulations were performed for various types of surfaces (ground, polished etc.) with and without several types of reflectors (paint, metal, teflon with air gap). For the continuous scintillator design, the sides will be blackened (absorbing) to provide uniformity of light spread for positioning [3,4]. This blackening is unnecessary for the segmented positioning situation since the scintillator-fiber units in the bundle are independent of each other. For the other two sides of the scintillator, top (facing the radiation) and back (facing the fibers) different surface treatments produced significantly different results. Figure 4 shows the simulated light yield obtained for various surface treatments of the scintillator top for the 2 and 12.5 mm diameter plastic (1.25 mm thick) and $CaF_2(Eu)$ (0.7 mm thick) scintillators. In all cases, the best conditions obtained were a ground surface painted with a diffuse reflector. For the back (PMT) end of the scintillator, ground or polished surfaces tended to produce similar results.

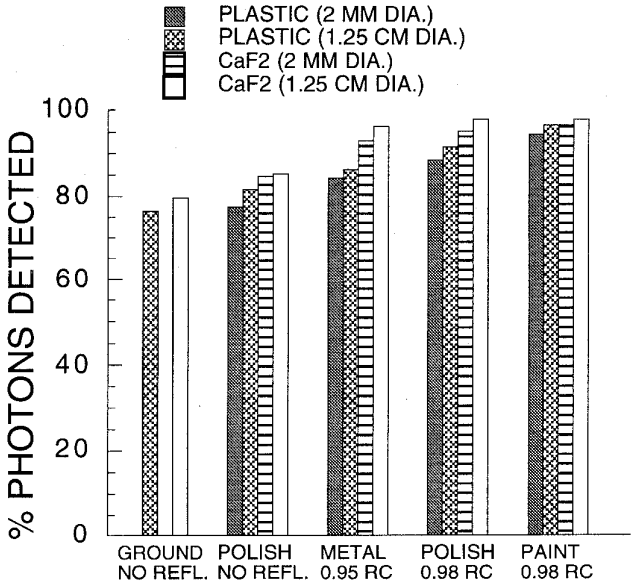

Fig. 4. Simulated scintillation light yield for various top surface treatments (RC=reflection coefficient) for plastic and $CaF_2(Eu)$ scintillators of 1.2 and 0.7 mm thick, respectively. Diameters are shown at top. For the metal reflector case, a polished surface is assumed. The best top surface treatment found was ground and painted with a diffuse reflector with a high RC (far right).

Figure 5 shows the simulated light output for various plastic scintillator thicknesses (2 mm dia.) with and without 5 cm plastic fiber (n_{core}=1.6, n_{clad}=1.49) coupling to a PMT. The simulated scintillator was ground and painted with a diffuse reflector on the top and polished on the sides. There is significant difference in light transmission vs length (as large as 30% from 0.5 to 3 mm thickness) when the scintillator is

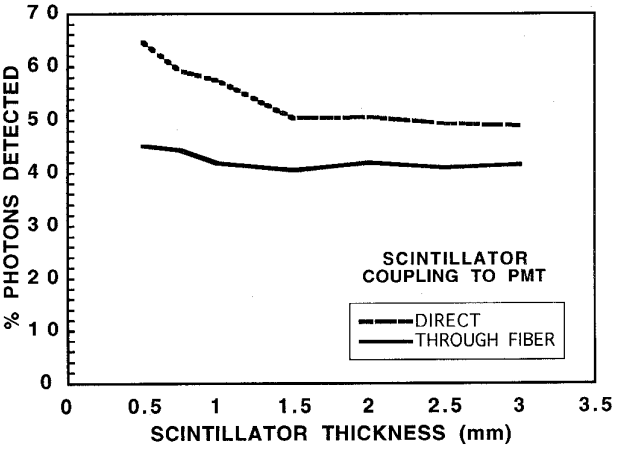

Fig. 5. Simulated light yield vs. scintillator thickness (2 mm diameter plastic). $CaF_2(Eu)$ showed the same trend. The clear fiber coupling (5 cm) removes the dependence of light yield on thickness. The 1.25 cm diameter scintillators with or without coupling to a fiber bundle, showed similar trends.

coupled directly to the PMT. The figure shows results for 2 mm diameter plastic but similar trends were found for the 1.25 cm diameter case (with and without the 19 fiber bundle) except with a less dramatic rise for the directly coupled case [5]. This effect is probably a combination of improved acceptance angle into the PMT and less side reflections for thinner detectors (light attenuation due to side reflections goes as the length divided by the cross-sectional area). This variation in light collection is not seen when fiber coupling is used. The fiber effectively acts as a light collimator by only transmitting those light rays whose entrance angle meets the fiber's criteria for total internal reflection. Similar results were found with simulations using BCF-10 scintillating fiber (outer clad about a scintillating core).

Figure 6 shows the light yield as a function of refractive index of the 0.1 mm thick coupling compound between the scintillator (2 mm dia.) and a 5 cm long, 2 mm diameter fiber (n_{core}=1.6, n_{clad}=1.49). The attenuation length of the fiber core and clad was set at 2 m. Over the index of

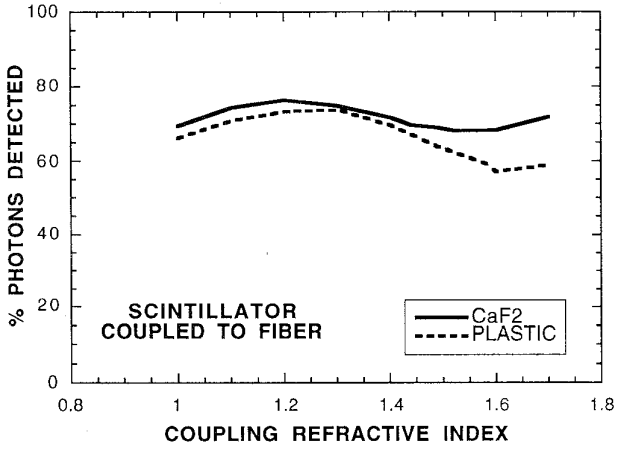

Fig. 6. Simulated scintillation light yield as a function of refractive index of the optical coupling compound used to couple a 2 mm diameter scintillator (with or without cladding) to fibers.

refraction range studied there is little variation in yield for CaF_2(Eu) and moderate variation for the plastic scintillator coupled to fiber. The reason for this non-intuitive weak dependence is most likely due to the finite angular cone of acceptance (numerical aperture) for the fiber. Regardless of the index of refraction of the scintillator-fiber interface, large angles of entrance into the fiber are not transmitted. Only forward directed light will be transmitted down the fiber. Thus, the index of refraction mismatch between the scintillator and fiber does not play as big a role in fiber-coupled systems. With direct (without fiber) coupling to the PMT, the best coupling refractive index in the simulations was at the geometrical mean of the scintillator and the PMT glass window.

The simulation of Figure 7 shows that the amount of light detected increases with the numerical aperture (NA) of a fiber. A PMMA fiber cladding with 1.49 refractive index is assumed and the core index is varied. For short fiber lengths, significant transmission of light occurs in the cladding as well as the core of the fiber. A clear fiber with large NA should be chosen.

To facilitate light sharing in the continuous positioning detector a light diffuser is required. The thickness

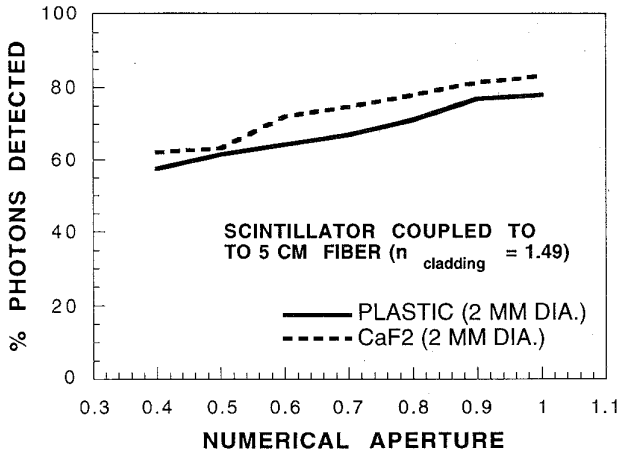

Fig. 7. Simulated scintillation light yield when coupled to a 5 cm long clear fiber as a function of the numerical aperture of the fiber.

of the light diffuser required for the best image uniformity and continuity was determined [3,4] to be just below 2 mm. The presence of a light diffuser introduces an extra coupling interface between the continuous scintillator and fiber bundle. Figure 8 indicates that the refractive index of the light diffuser should be high for best transmission. Assuming a polystyrene diffuser (n=1.58) the yield as a function of the refractive index of the coupling interface between the scintillator and diffuser

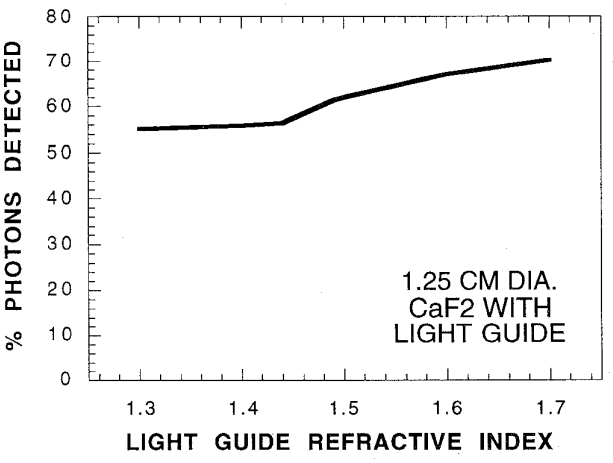

Fig. 8. Simulated scintillation light yield of a 1.25 cm diameter, 0.7 mm thick CaF_2(Eu) disk coupled to a 2 mm thick light diffuser as a function of light diffuser index of refraction (no fibers).

did not change significantly. The index of refraction of the interface between light diffuser and fiber was more important. Figure 9 shows the simulated optical transmission for several choices of light diffusers as a function of the refractive index of the second (light diffuser/fiber) interface (n = 1.49 coupling refractive index at the scintillator light diffuser interface, same clear fibers as used for Fig. 6.). The best response was obtained at a refractive index between 1.5 and 1.6 (the geometrical mean). The low index of refraction of CaF_2(Eu) (n=1.44) facilitates optical coupling to a light diffuser (n=1.58) and/or optical fibers (n=1.6 core) (at each interface, the transmitted light will be refracted towards smaller angles with respect to the fiber axis).

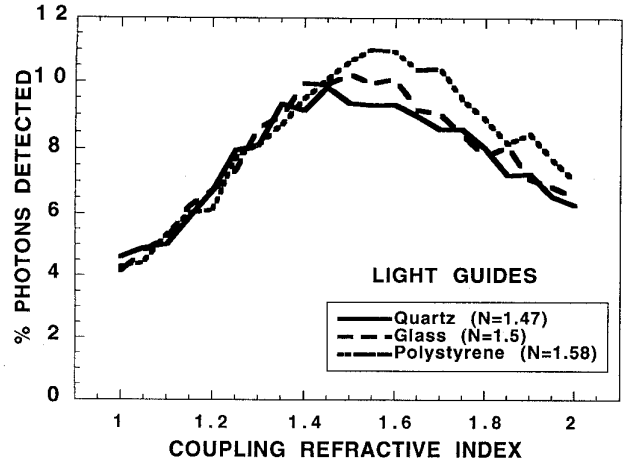

Fig. 9. Continuous detector scintillation light yield as a function of refractive index of light diffuser/fiber interface for different light diffuser materials.

Another factor that was studied was the use of various holders for the fiber bundle (see Fig. 1). The best light output was obtained using white Lucite as the material [4]. Using aluminum and black Lucite holders caused as much as 15 and 30% lower yield, respectively, probably due to their increased absorption of cladding light (remember, for short fiber lengths, cladding light can be significant).

C. Experimental Data: Scintillators for the Segmented Imaging Array

Figure 10 shows typical beta spectra measured for two different scintillator thicknesses of BC404. We used the weighted mean (centroid) of a ^{204}Tl beta spectrum (E_{max} = 765 keV, similar to that of ^{18}F, without the annihilation photons) as a measure of the light output of the scintillator.

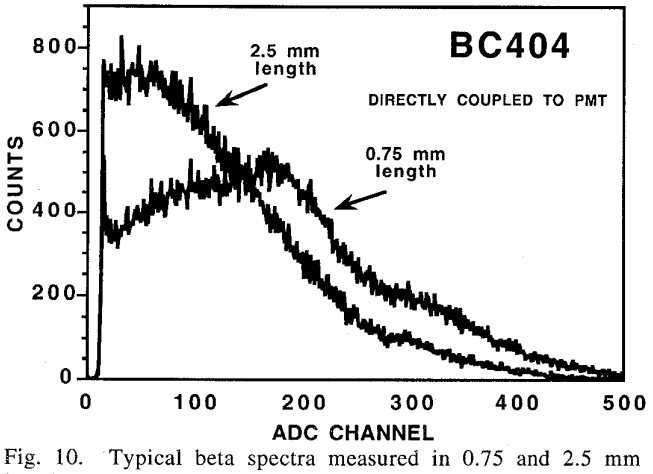

Fig. 10. Typical beta spectra measured in 0.75 and 2.5 mm lengths of 2 mm diameter BC404 scintillator directly coupled to a PMT. The relative light yield is measured by the spectrum weighted mean.

Figures 11 and 12 show the results of light output measurements performed using 2 mm diameter pieces of the plastic scintillator, coupled either directly onto a PMT, or indirectly through a 5 cm long piece of 2 mm diameter clear fiber (Pol. Hi.Tech, NA = 0.57). Each point represents the mean and standard deviation of at least four separate measurements. For these studies no reflectors were used and all surfaces were polished. Two competing physical effects that are dependent on scintillator thickness are demonstrated in these figures: electron absorption and light transmission probabilities. For the scintillator directly coupled to the PMT (Fig. 11), the light yield increases systematically as the thickness of the scintillator decreases, until approximately 1.0 mm, where it begins to decrease. There is a 30% difference in light output between the 0.75 and 3 mm thicknesses. When coupled to the PMT through a 2 mm diameter, 5 cm long clear fiber (Fig. 12), the thicknesses dependence of the light yield is removed. In the direct-coupled case, the solid angle of acceptance of scintillation light into the PMT improves (explaining the increase) as the thickness of the scintillator is decreased. With fiber-coupling, there is only roughly a 42° light acceptance cone for internally reflected light (determined by the fiber numerical aperture) and, hence, solid angle effects due to proximity are removed. These results compare well to the Monte Carlo study shown in Section IIIB, Figure 5 down to approximately 1 mm.

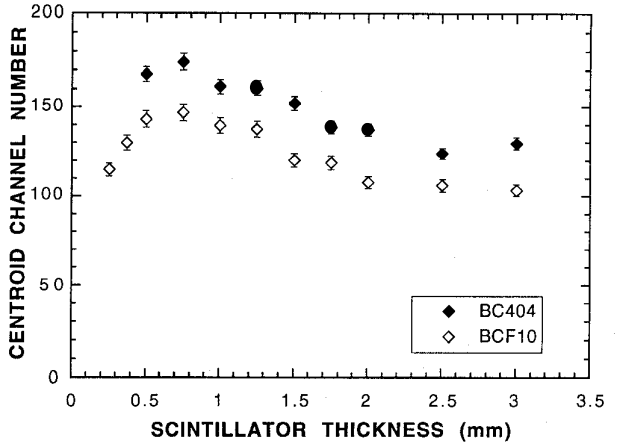

Figure 11. Light output measured for 2 mm diameter plastic scintillators directly coupled to a PMT as a function of scintillator thickness for flood beta irradiation from ^{204}Tl.

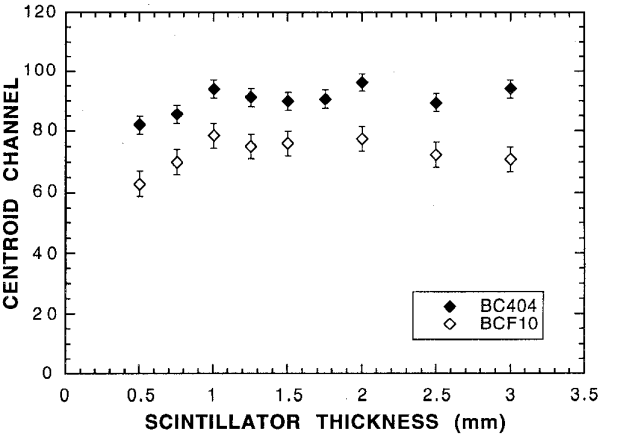

Figure 12. Light output measured for 2 mm diameter plastic scintillators coupled via a 5 cm length of clear fiber to a PMT as a function of scintillator thickness.

The competing effect of incomplete energy deposition begins to play a role in Figs. 11 and 12 for thicknesses near and below 1 mm, where the light output begins to decrease. Below 0.7 mm thickness we observed a rapid drop in light output due to beta penetration. The resulting measured data as a function of thickness is a convolution of the probabilities of beta energy absorption (which increases with increasing thickness; see simulation, Fig. 2) and light transmission (which increases with decreasing thickness; see simulation, Fig. 5).

There was a factor of 4.4 difference in light output measured between direct and fiber coupling to the PMT (Figures 11 and 12 have a factor of 2.5 difference in scale; the amplifier gain was 2.5 times higher for the data taken in Figure 12). The difference between direct and fiber coupling was not so drastic in the simulations of Figure 5. This discrepancy might be explained by the fact that perfect surfaces were assumed in the simulations. In reality the surfaces have flaws and non-uniformities. For example, for clad fibers, significant differences in light output were observed in simulations between the cases of ground or polished clad surfaces. This is especially true for a 5 cm fiber length where cladding light transmission is significant.

From Figures 11 and 12 it is also seen that BC404 has systematically 20-25% more light output than the BCF-10 scintillating fiber of the same outer diameter for these short thicknesses (for the bialkali photocathode tube used). This corresponds to the intrinsically higher light output in the PVT base than for Polystyrene (see Table 1) and the absence of the clad and therefore larger effective cross-sectional area of the PVT. $CaF_2(Eu)$ was unavailable in the 2 mm diameter dimension for comparison.

D. Experimental Data: Scintillators for the Continuous Imaging Detector

In the last sub-section and in simulations (Fig. 5) we saw that fiber coupling removes the thickness dependence of the scintillation light yield (above the beta penetration threshold thickness). The same effect was seen for 1.25 cm diameter continuous scintillators with fiber bundle coupling. We will concentrate on the fiber coupling data in this subsection and examine the effect of different surface reflectors. Figure 13 shows the results measured for 1.25 cm diameter disks of BC404 and $CaF_2(Eu)$ coupled to a hexagonal-packed bundle of nineteen, 2 mm diameter clear fibers (Bicron BCF-98) for different top reflectors. For BC404, the light output varies with thickness in a similar manner to that seen in Figure 12, while for $CaF_2(Eu)$ the saturation appeared near 0.5 mm (only 3 $CaF_2(Eu)$ thicknesses were available). We measured that the $CaF_2(Eu)$ system produced on average three times the light of BC404 (for a bialkali PMT). This is consistent with the differences in light output and index of refraction between $CaF_2(Eu)$ and BC404 (see Table 1). The low index of refraction of $CaF_2(Eu)$ facilitates coupling to the clear plastic fiber (NA=0.57). Figure 13 (bottom) shows the degradation in light yield (downward shift in beta spectrum mean) expected with a 1.25 cm diameter $CaF_2(Eu)$ disk (1 mm thick) coupled to a 5 cm long fiber bundle of 19, 2 mm diameter clear fibers.

The result of using various reflector materials is also shown in Figure 13. As predicted from DETECT simulations (Section IIIB), the best reflector found was a white diffuse reflector (Teflon) which was measured to produce nearly twice the light output than for the case without reflectors. We also investigated the use of white TiO_2 reflecting paint and saw only slightly greater light output to that measured using teflon. The reflector must be opaque in order to minimize light leak (internal and ambient), yet be thin and non-absorbing

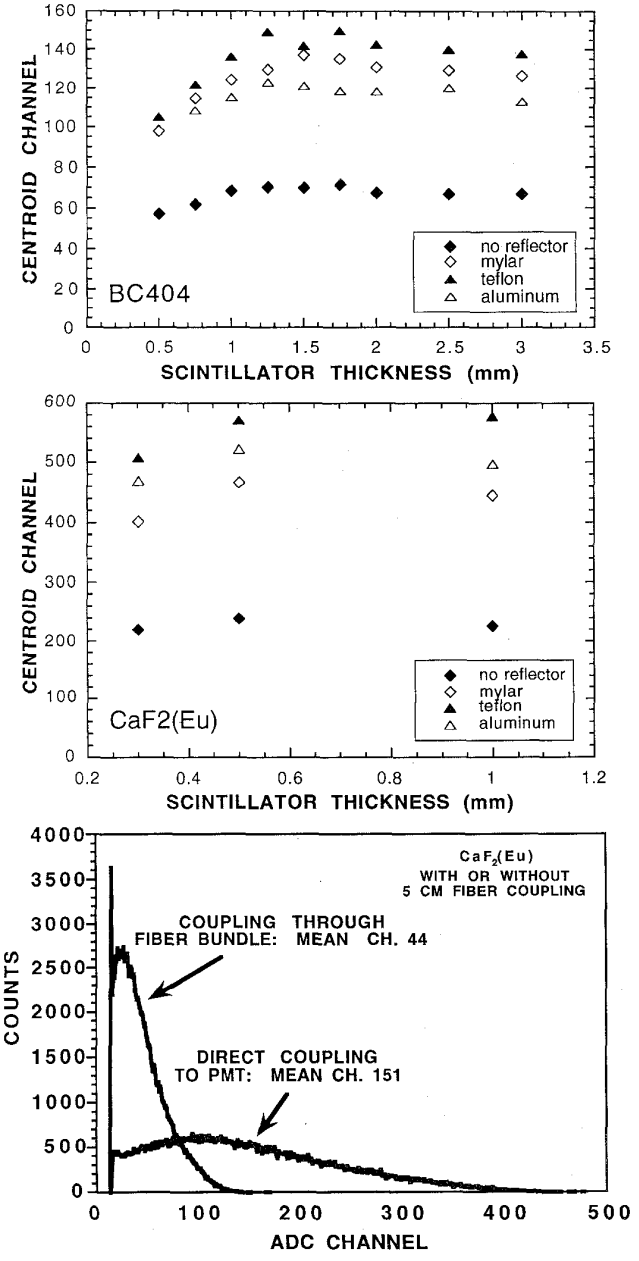

Fig. 13. Measured ^{204}Tl spectrum centroid as a function of scintillator thickness for 1.25 cm diameter (top) BC404 and (middle) $CaF_2(Eu)$ scintillators coupled to a bundle of 19, 5 cm long 2 mm diameter clear plastic fibers for different top surface reflectors. The two data sets are plotted on the same scale for comparison. Bottom: a factor of 3-4 light loss (downward shift in beta spectrum mean) occurs with the fiber bundle coupling (a white teflon reflector was used and all surfaces were polished).

of beta particles. We investigated the use of more than one layer of teflon and saw a slight degradation in light output. Electron energy loss in multiple reflector layers seemed to play a larger role in light output than does the higher reflectivity.

The light collection improved with the choice of the clear fiber. Transmission properties of several quartz, glass and plastic fibers with various numerical apertures (NA) were studied with the scintillators attached [4]. We found a double clad Kuraray fiber (NA = 0.72) to produce the best combination of high light output and sensitivity (total # beta events detected per unit time). A bundle of 19, 2 mm double-clad Kuraray fibers transmitted approximately 30% more light for our configuration than the single-clad Bicron (BCF-98) fibers. After calibration with an LED (described in [5]) we found that the continuous $CaF_2(Eu)$/fiber bundle system (1.25 cm dia., 0.5 mm thick $CaF_2(Eu)$ with 2 mm dia. double clad Kuraray 19-fiber bundle) produced on average ~250 photoelectrons at the PMT photocathode for the ^{204}Tl electron spectrum. This number of photons is sufficient for < 1 mm positioning [8] using multi-channel photodetectors.

E. Segmented vs Continuous Positioning Camera

The choice between the segmented or continuous camera depends on several factors. Figure 14 shows a measured comparison between the light output from a 2 mm diameter piece of BC404 coupled to a 5 cm length of 2 mm diameter fiber and that from a 1.25 cm diameter disk of BC404 coupled to a bundle of 19 of the same fibers (the scintillators were 1.25 mm thick). The fiber coupling efficiency is greater for the former case with a 25% greater scintillation light yield than for the latter (using the same lower energy threshold for the centroid calculation). The 2 mm thick light guide (diffuser) required for light spread in the continuous positioning case will introduce an additional reduction in light yield of 20% [4].

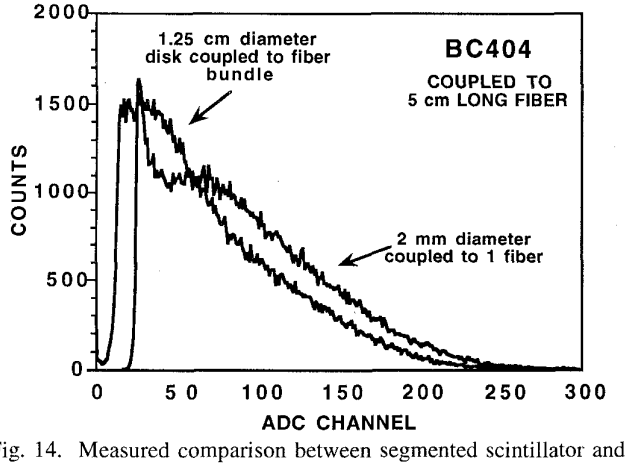

Fig. 14. Measured comparison between segmented scintillator and continuous positioning designs (BC404, 1.25 mm thickness, 2 and 12.5 mm diameters). Because the fiber bundle coupling has some light transmission dead area in the continuous design, the light output for the segmented array is higher (see Fig. 1).

IV. DISCUSSION

The design we have chosen for the beta-ray intraoperative imaging probe requires a long (~2 m) plastic optical fiber bundle scintillation light readout to allow flexibility for the surgeon and to completely isolate the electronics from the patient during surgery. Because of this fiber-coupled design it is crucial that as many scintillation photons be collected by the photodetector as possible. Due to the small thicknesses of the scintillators required for beta detection, light collection efficiency from the scintillator into the fiber bundle is high.

We have studied light output for various scintillator materials and geometries, reflectors and clear fiber light guides. The choice of the scintillator somewhat depends on the type of photodetector to be used. For the prototype VLPC segmented imaging probe, 3HF scintillating fiber was chosen [1,2] for its high emission wavelength (535 nm and, therefore, good spectral match with the absorption spectrum of the VLPC [1,2]). For the MA-PMT version of the beta camera [3,4], $CaF_2(Eu)$ was the scintillator of choice because of its high light output, low index of refraction (compared to core of the fiber), good spectral match with bialkali phototubes, high stopping power for beta particles in the energy range of interest (0-635 keV), and transparency to 511 keV photons (low Z and density). A $CaF_2(Eu)$ thickness of ~0.5-0.7 mm was chosen for high scintillation light yield and low gamma-ray efficiency.

Energy deposition and light transmission were seen to compete with one another for scintillator thicknesses on the order of the beta range in that material. The measured response was observed to be convolution of these two physical components. From our measurements we saw that fiber coupling reduces the dependence of scintillation light yield on thickness except for thicknesses roughly below the beta range. White reflecting paint with 0.98 reflectivity was chosen since it produced the best scintillation light signal and it is simple to use. A clear plastic fiber (Kuraray, NA=0.72) was chosen for the front end fiber readout of the scintillator.

With the $CaF_2(Eu)$ system we measured a mean of ~250 photoelectrons per event at the photocathode of the PMT. This number of photoelectrons is sufficient for <1 mm positioning resolution [4,8]. For the continuous scintillator imaging probe it is necessary to have a suitable light diffuser (roughly 1.7 mm thick) coupled to the back of scintillator to spread the scintillation light among the fibers in the bundle for positioning. Polystyrene (n=1.58) was chosen for the light diffuser. Without this light diffuser the fiber bundle granularity will be seen in the resulting images [4]. This light diffuser degraded light yield by ~25%. If desired, the light sharing could be performed without introducing a light diffuser by increasing the scintillator thickness at the expense of increasing background. We will further discuss the topic of background in later work.

Whether one uses a continuous or segmented scintillator for the camera depends on several considerations. In terms of light yield and energy resolution the segmented version of the camera (see Fig. 14), with 19 independent scintillator-fiber units may be superior. However, in that case the image resolution (pixel size) is determined by the diameter of each individual scintillator unit in the array, in this case 2 mm. One may then want to reduce the scintillator diameter, which means increasing the number of elements in the array in order to cover the same imaging area, which in our prototype design is 1.2 cm^2 (~1.25 cm total scintillator diameter). However, the scintillator diameter should not be smaller than that required to stop the average beta.

With the continuous positioning camera, the positioning is accomplished through light sharing among the fibers in the bundle (the fibers are, thus interdependent) and a weighted mean of the individual fiber signals. In principle, the image resolution is limited only by the number of scintillation light photons produced and distributed into the fibers in the bundle. We have found the resolution to be significantly better than the 2 mm diameter clear fiber size [3,4]. In addition, because of the lower packing fraction in the segmented array (unless square pieces are used) the overall efficiency and sensitivity is better for the continuous scintillator.

V. ACKNOWLEDGMENTS

The authors thank Ken Meadors for technical assistance. This research was supported by NIH Grants T32 CA09092 and R01-CA61037 and DOE Grant DE-FC03-87-ER 60615.

VI. REFERENCES

[1] LR MacDonald, MP Tornai, CS Levin, J Park, M Atac, DB Cline and EJ Hoffman. Investigation of the Physical Aspects of Beta Imaging Probes Using Scintillating Fibers and Visible Light Photon Counters. *IEEE Trans. Nucl. Sci.* **42-4**, August 1995, 1351-7.

[2] LR MacDonald, MP Tornai, CS Levin, J Park, M Atac, DB Cline and EJ Hoffman. Small area, fiber coupled scintillation camera for imaging beta-ray distributions intra-operatively. *Photoelectronic Detectors, Cameras and Systems*, CB Johnson, EJ Fenyves, Editors, *Proc. SPIE* **2551**, 92-101 (1995).

[3] MP Tornai, CS Levin, LR MacDonald, EJ Hoffman, J Park, M Atac. Development of a Small Area Beta Detecting Probe for Intra-Operative Tumor Imaging. *J. Nucl. Med.* **36**, 1995, p. 109.

[4] MP Tornai, LR MacDonald, CS Levin, S Siegel, EJ Hoffman. Design Considerations and Initial Performance of a 1.2 cm^2 Beta Imaging Intra-operative Probe. Submitted to *IEEE Trans. Nucl. Sci.*

[5] MP Tornai, EJ Hoffman, CS Levin, LR MacDonald. Optimization of Fluor Concentration in a New Organic Scintillator for In Situ Beta Imaging. Submitted to *IEEE Trans. Nucl. Sci.*

[6] GF Knoll, TF Knoll, TM Henderson. Light Collection in Scintillating Detector Composites for Neutron Detection. *IEEE Trans Nucl Sci*, NS-**35**, 1988, p.872-875.

[7] Stanford Linear Accelerator Center (1991).

[8] E Tanaka, T Hiramoto and N Nahara. Scintillation Cameras based on New Position Arithmetics. J. Nucl. Med. **11-9** (1970)542-547.